The mRNA-binding protein IGF2BP1 maintains intestinal barrier function by up-regulating occludin expression

Received for publication, March 28, 2020, and in revised form, May 1, 2020 Published, Papers in Press, May 8, 2020, DOI 10.1074/jbc.AC120.013646

Vikash Singh[1], Chethana P. Gowda[1], Vishal Singh[2], Ashwinkumar S. Ganapathy[3], Dipti M. Karamchandani[4], Melanie A. Eshelman[5], Gregory S. Yochum[5,6], Prashant Nighot[3], and Vladimir S. Spiegelman[1,*]

From the [1]Division of Hematology and Oncology, Pediatric Department, and the Departments of [3]Medicine, [4]Pathology, [5]Biochemistry & Molecular Biology, and [6]Surgery, Pennsylvania State College of Medicine, Hershey, Pennsylvania, USA and the [2]Department of Nutritional Sciences, Pennsylvania State University, University Park, Pennsylvania, USA

Edited by Ronald C. Wek

Insulin-like growth factor 2 mRNA-binding protein 1 (IGF2BP1) is an mRNA-binding protein that has an oncofetal pattern of expression. It is also expressed in intestinal tissue, suggesting that it has a possible role in intestinal homeostasis. To investigate this possibility, here we generated Villin CreERT2: Igf2bp1flox/flox mice, which enabled induction of an IGF2BP1 knockout specifically in intestinal epithelial cells (IECs) of adult mice. Using gut barrier and epithelial permeability assays and several biochemical approaches, we found that IGF2BP1 ablation in the adult intestinal epithelium causes mild active colitis and mild-to-moderate active enteritis. Moreover, the IGF2BP1 deletion aggravated dextran sodium sulfate–induced colitis. We also found that IGF2BP1 removal compromises barrier function of the intestinal epithelium, resulting from altered protein expression at tight junctions. Mechanistically, IGF2BP1 interacted with the mRNA of the tight-junction protein occludin (Ocln), stabilizing Ocln mRNA and inducing expression of occludin in IECs. Furthermore, ectopic occludin expression in IGF2BP1-knockdown cells restored barrier function. We conclude that IGF2BP1-dependent regulation of occludin expression is an important mechanism in intestinal barrier function maintenance and in the prevention of colitis.

Insulin-like growth factor 2 mRNA–binding protein 1 (IGF2BP1, also known as CRD-BP/ZBP1/IMP1/VICKZ1) is a protein with an oncofetal pattern of expression exhibiting higher levels in fetal and neonatal tissues and low levels in adult tissues and is re-expressed in a variety of cancers (1, 2). IGF2BP1 binds a diverse set of mRNAs, affecting their stability and subcellular localization (3, 4). Well-established mRNA targets of IGF2BP1 include c-*MYC*, *βTrCP1*, *GLI1*, *MITF*, *MDR1*, *H19*, *CD44*, and *PTGS2* (5–16). IGF2BP1 is also known to regulate cellular polarity and cell migration by escorting its target mRNAs to their proper subcellular site of protein synthesis (8, 10, 17). Photoactivatable ribonucleoside–enhanced cross-linking and immunoprecipitation (PAR-CLIP) and enhanced cross-linking and immunoprecipitation (eCLIP) experiments identified additional IGF2BP1 targets, suggesting its role in a multitude of cellular processes (18, 19). Identification of IGF2BP1 as a reader of N^6-methyladenosine modification further added a new dimension to its regulatory function (20, 21).

Intestinal epithelial cells (IECs) establish and maintain a barrier to separate the submucosa from the intestinal lumen (22). This epithelial integrity is controlled by the junction complex comprised of the tight junction (TJ) and the adherent junction (23). The principle determinant of intestinal permeability and *trans*-epithelial transport is the TJ complex. Disrupted TJ and increased intestinal permeability may lead to intestinal inflammation (23, 24). Occludin is one of the key TJ proteins that contributes to the maintenance of an intact intestinal epithelium. Interestingly, *Ocln* mRNA is unstable and has been shown to undergo post-transcriptional regulation (23, 25, 26).

Inflammatory bowel disease (IBD) is a chronic inflammatory condition of the intestine and can manifest severe chronic active mucosal injury with restricted therapeutic options (27, 28). There are two main types of IBD, Crohn's disease and ulcerative colitis (29). One of the major factors in the development of IBD is the loss of intestinal epithelial barrier function, which elicits an inflammatory response that contributes to further barrier disruption (29). IGF2BP1 hypomorphic mice manifested various developmental defects and embryonic lethality (2). The intestine of these mice displayed abnormal crypt and villous architecture indicating a role for IGF2BP1 in intestinal development. Moreover, the role of IGF2BP1 was also implicated in healing of a mechanical wound across an epithelial monolayer of cells (11, 30). Interestingly, the deletion of IGF2BP1 in intestinal epithelial cells was recently shown to ameliorate experimental colitis in mice (31). Together, these findings hint to the function of IGF2BP1 in maintaining intestinal homeostasis.

For the current study, we generated mice that allow inducible knockout of IGF2BP1 specifically in the adult intestinal epithelium to study pathological processes independent of potential developmental defects. Here, we demonstrate that the ablation of *Igf2bp1* in adult IECs leads to acute colitis in mice, and IGF2BP1 deficiency in IECs decreases occludin levels, resulting in a defective barrier function. These findings uncover an important function of IGF2BP1 in IECs to protect against colitis.

Results and discussion

Deletion of IGF2BP1 in IECs leads to acute colitis in mice

To investigate the role of IGF2BP1 in intestinal homeostasis, we generated *Villin-CreER^{T2}-Igf2bp1$^{fl/fl}$* transgenic mice. In these

This article contains supporting information.

* For correspondence: Vladimir S. Spiegelman, vspiegelman@pennstatehealth.psu.edu.

mice, transient knockout of *Igf2bp1* (hereafter, *Igf2bp1*$^{\text{IEC-Ind KO}}$) is induced via tamoxifen. Immunoblotting with anti-IGF2BP1 antibody was performed to confirm the ablation of Igf2bp1 from intestinal epithelium cells of *Igf2bp1*$^{\text{IEC-Ind KO}}$ mice (Fig. 1*A*). Intriguingly, adult *Igf2bp1*$^{\text{IEC-Ind KO}}$ mice displayed loss in body weight compared with *Igf2bp1*$^{fl/fl}$ littermates (Fig. 1*B*). Next, we examined the gross appearance of intestine and length of colon to inspect colon shortening, which is considered as the indicator of inflammation. In our analysis, we did not observe any significant change in gross appearance of intestine and in colon length of *Igf2bp1*$^{\text{IEC-Ind KO}}$ mice (Fig. 1*C*). Histological analysis of small intestines revealed that all *Igf2bp1*$^{\text{IEC-Ind KO}}$ mice exhibited increased lamina propria cellularity with mild to moderate active enteritis and patchy to diffuse neutrophilic and lymphocytic infiltration, when compared with control mice (Fig. 1*D* and Fig. S1*B*). Likewise, the colons of *Igf2bp1*$^{\text{IEC-Ind KO}}$ mice displayed mild active colitis with increased lamina propria cellularity and mild to moderate patchy to diffuse neutrophilic and lymphocytic infiltration. At places, there were loss of crypts with abscess formation (Fig. 1*D* and Fig. S1*A*). Based on the hematoxylin/eosin (H&E)-stained sections, analyzed by the pathologist in blinded manner, the samples were scored on two major histomorphological criteria: (i) severity of inflammatory cell infiltrates and (ii) epithelial changes (cryptitis, crypt abscesses, and erosion) (Fig. 1*E*). These results illustrate the importance of epithelial IGF2BP1 for normal intestinal physiology.

IGF2BP1 deficiency sensitizes mice to dextran sodium sulfate-induced colitis

Next, we examined whether induced intestinal epithelial IGF2BP1 knockout affects sensitivity of mice to DSS, which is a toxic chemical that when delivered in the drinking water causes colitis by disrupting the intestinal epithelium. Here we performed chronic DSS treatment as it is the most relevant model for experimental colitis in mice. In the first cycle of this experiment, mice were treated with 2% DSS for 5 days, followed by intermittent periods of normal drinking water. This cycle was repeated two more times, and mice were then euthanized and examined. This experiment conferred 75% mortality in *Igf2bp1*$^{\text{IEC-Ind KO}}$ mice (Fig. 2*A*). We also observed significant loss in weight and increases in disease activity index (DAI) scores (32) in *Igf2bp1*$^{\text{IEC-Ind KO}}$ mice when compared with control littermates (Fig. 2, *B* and *C*). As severe chronic inflammation is known to decrease colon lengths, we evaluated colons at the conclusion of the experiment and found significantly shorter colons in *Igf2bp1*$^{\text{IEC-Ind KO}}$ mice than in the control littermates (Fig. 2*D*). We have also analyzed the H&E-stained sections of these colons and observed that the colon sections from DSS-treated *Igf2bp1*$^{\text{IEC-Ind KO}}$ mice showed increased disruption of colonic mucosa along with crypt abscesses, loss of colonic surface epithelium and crypts, and diffuse infiltration of inflammatory cells when compared with control mice (Fig. 2*E* and Fig. S1*C*). These tissue sections were analyzed and histomorphologically scored based on established criteria (Fig. 2*F*) (33, 59). These results indicate that IGF2BP1$^{\text{IEC-Ind KO}}$ mice are more sensitive to DSS challenge and develop more disease-related phenotypes in the intestine.

IGF2BP1 deficiency increases intestinal permeability by affecting the occludin expression in IECs

The intact epithelium imparts a protective barrier against entry of foreign antigens from the intestinal lumen into the lamina propria. The aforementioned data suggest that IGF2BP1 may be important for maintaining barrier function of intestinal epithelium. To assess the permeability of intestine, we extracted serum from blood for quantifying specific IgG levels by ELISA. We found elevated levels of IgG to LPS (serological bacterial marker) in the serum of *Igf2bp1*$^{\text{IEC-Ind KO}}$ mice, which was indicative of increased intestinal permeability (Fig. 3*A*). To confirm these results, we used the FITC-dextran permeability assay, which is a classical method for evaluating the status of intestinal barrier function. Four hours after oral administration of FITC-dextran, we isolated serum and examined the level of FITC-dextran in the samples. Significantly higher levels of FITC-dextran were found in *Igf2bp1*$^{\text{IEC-Ind KO}}$ mice compared with *Igf2bp1*$^{fl/fl}$ littermates (Fig. 3*B*). These results indicate that IGF2BP1 is involved in the maintenance of intestinal barrier function, and its absence disrupted the barrier.

A disrupted TJ is a major cause of intestine barrier dysfunction (34), and this motivated us to investigate the levels of major TJ proteins in IECs of *Igf2bp1*$^{\text{IEC-Ind KO}}$ mice. We found decrease specifically in the levels of occludin TJ protein in the IECs from the intestines of *Igf2bp1*$^{\text{IEC-Ind KO}}$ mice, whereas other TJ proteins, CLAUDIN-1, CLAUDIN-2, ZO-1, and ZO-3, remained unaffected when compared with control littermates (Fig. 3*C*). Immunostaining analysis revealed significantly lower levels of occludin in colon IECs of *Igf2bp1*$^{\text{IEC-Ind KO}}$ mice when compared with control mice (Fig. 3*D*). These results suggest that IGF2BP1 affects the expression of occludin TJ protein and maintains intestine barrier function.

IGF2BP1 regulates occludin expression by directly binding to and stabilizing its mRNA

To investigate the mechanism of regulation of occludin TJ expression by IGF2BP1, we chose the human CCD841-CoTr normal colon epithelial cell line with moderate expression of Igf2bp1. Knockdown of IGF2BP1 using shRNAs in this cell line resulted in significant inhibition of occludin expression (Fig. 4*A*). IGF2BP1 is an RNA-binding protein (RBP) that often stabilizes its mRNA targets (6, 14), and to evaluate whether IGF2BP1 binds to the mRNA of occludin directly, we performed the CLIP assay. In our CLIP analysis, we found enrichment of *OCLN* mRNA to a similar extent as *bona fide* IGF2BP1 targets, such as *MYC* and *β-TRCP1* (Fig. 4*B*). To elucidate whether IGF2BP1 regulates the turnover of *OCLN* mRNAs, we performed an actinomycin D chase experiment in a pair of colorectal cell lines. The loss-of-function experiments (by knocking down IGF2BP1) were performed in Caco-2 cells characterized by high expression of IGF2BP1. The knockdown of IGF2BP1 and its effect on occludin expression were confirmed by immunoblotting (Fig. 4*C*). The actinomycin D chase experiments in Caco-2 cells showed that the knockdown of IGF2BP1 resulted in accelerated rate of *OCLN* mRNA degradation (Fig. 4*D*) but not of Claudin2 mRNA (Fig. S3*A*). The gain-of-

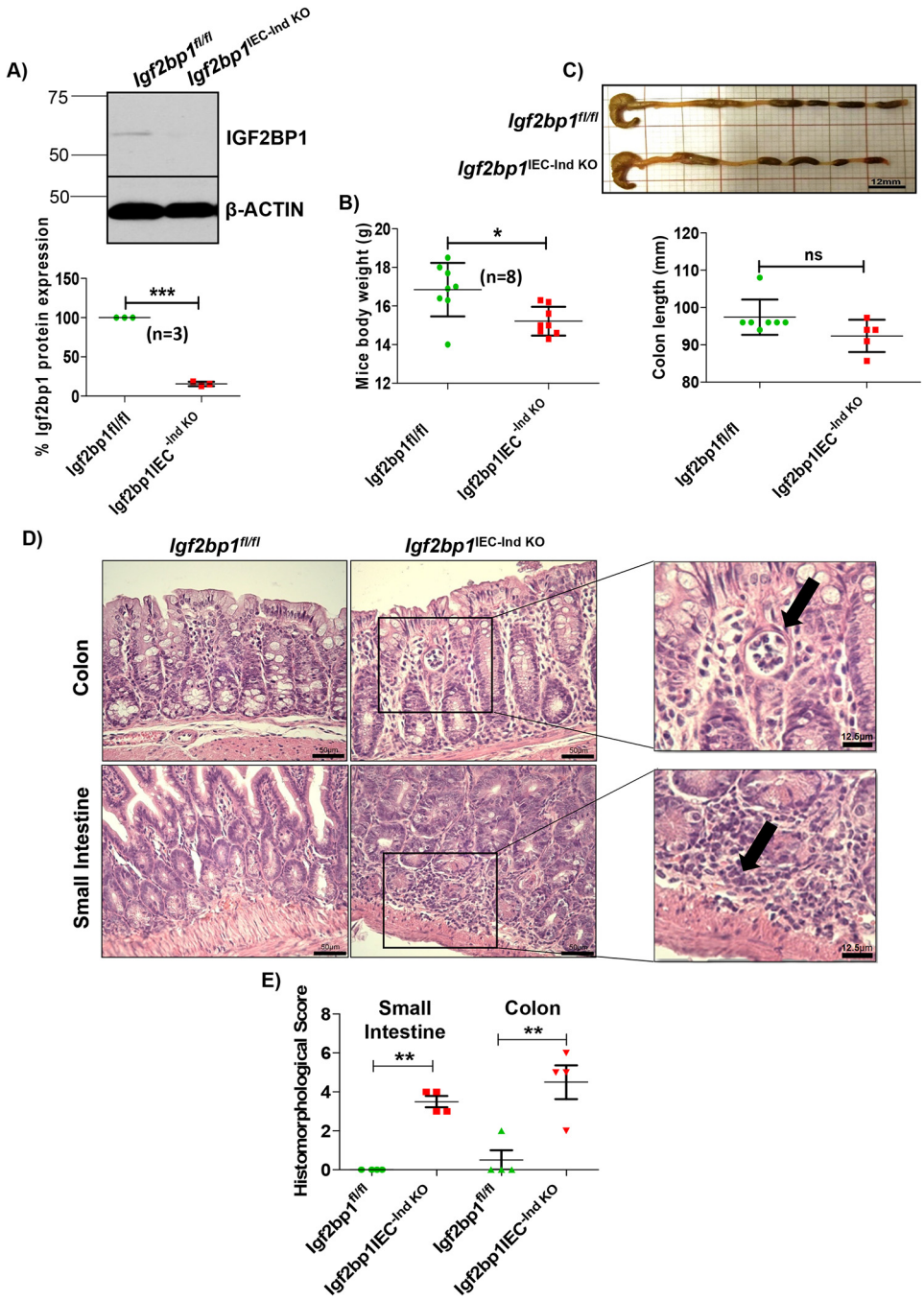

Figure 1. Induced deletion of IGF2BP1 in IECs confers acute mild colitis in mice. *A*, immunoblot in the *top panel* showing depletion of Igf2bp1 from intestinal epithelium cells of *Villin-CreER^{T2}-Igf2bp1$^{fl/fl}$* mice upon tamoxifen treatment. Signals are quantified in the *bottom panel* from three independent Igf2bp1 immunoblot analyses using ImageJ software. *B*, body weight of age-matched female (10–12-week) littermates after the induction of IGF2BP1 knockout from IECs. The data are means ± S.D. (*error bars*) ($n = 8$ for each genotype). *C*, colon length comparison after knocking out Igf2bp1. *Top*, representative image of colon from mentioned genotypes. *Scale bar*, 12 mm. *Bottom*, quantification of colon length. The data are means ± S.D. ($n = 7$ for *Igf2bp1$^{fl/fl}$* mice and $n = 5$ for *Villin-CreER^{T2}-Igf2bp1$^{fl/fl}$* mice). *D*, H&E-stained sections of colon and small intestine tissue from *Villin-CreER^{T2}-Igf2bp1$^{fl/fl}$* and control mice showing mild acute colitis and mild to medium acute enteritis. *Scale bars*, 50 μm (*micrograph*) and 12.5 μm (*inset*). *E*, histomorphological scores given to H&E-stained small intestine and colon tissue sections of *Igf2bp1$^{fl/fl}$* and *Villin-CreER^{T2}-Igf2bp1$^{fl/fl}$* mice by a sample-blinded pathologist for colitis and enteritis. Scores are provided to each sample based on general criteria of histomorphological characters reported previously (33, 59). *, $p < 0.05$; **, $p < 0.01$; ***, $p < 0.001$; *ns*, not significant.

function experiments (by overexpressing IGF2BP1) were performed in RKO cells that have negligible expression of endogenous IGF2BP1. Overexpression of IGF2BP1 protein in this cell line resulted in increased levels of occludin protein compared with control cells (Fig. 4*E*). Additional mRNA stability assays using these cells detected an increased $t_{1/2}$ of *OCLN* mRNA upon overexpression of IGF2BP1 (Fig. 4*F*), whereas there was no significant change in $t_{1/2}$ of Claudin2 mRNA (Fig. S3*B*). These results show that IGF2BP1 protein regulates occludin expression by directly interacting with *OCLN* mRNA and stabilizing it, establishing *OCLN* mRNA as a novel direct target of IGF2BP1.

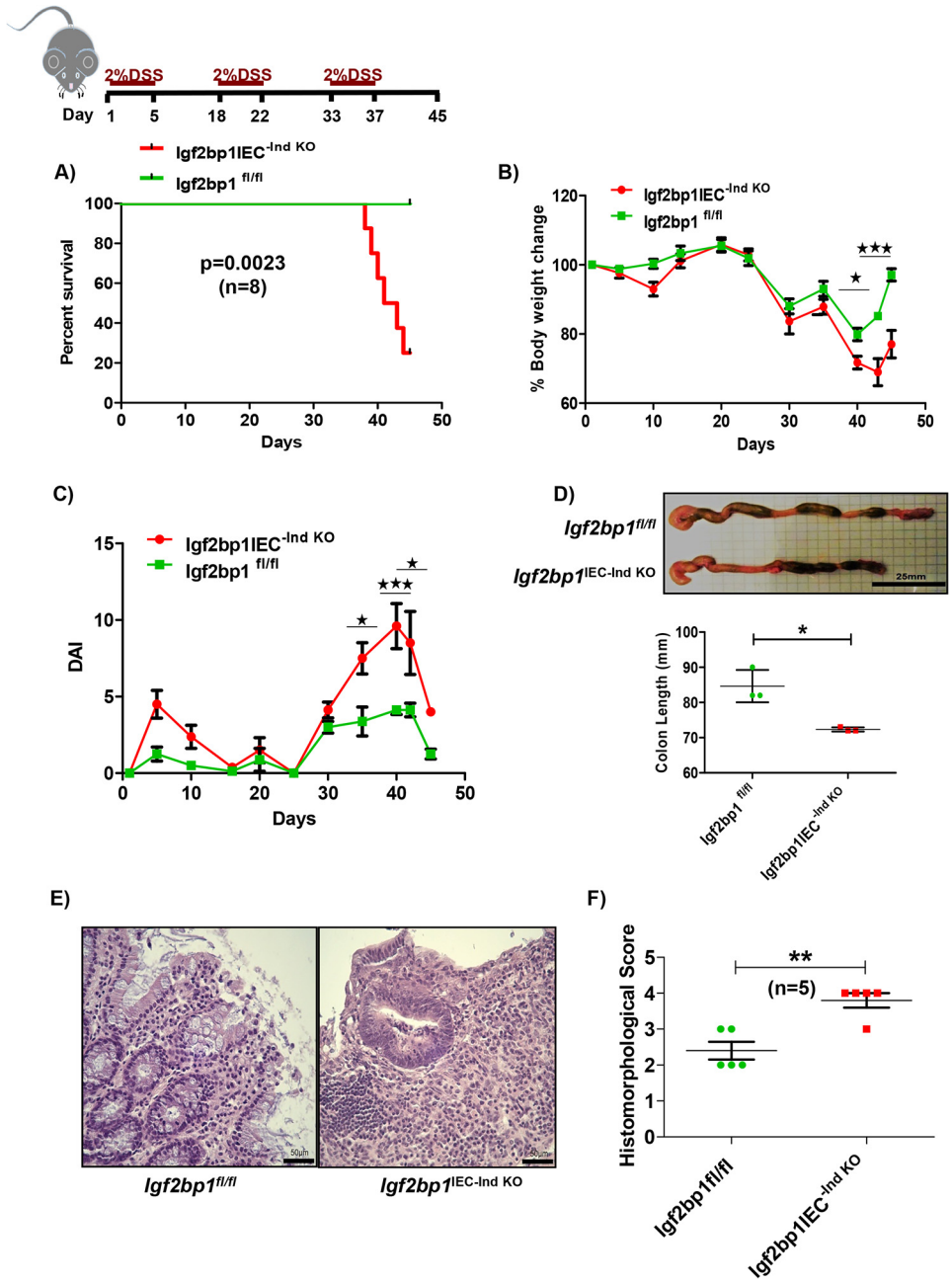

Figure 2. Deletion of IGF2BP1 sensitizes mice to DSS colitis. *A*, survival curve for chronic DSS treatment showing significant loss of mice in the *Villin-CreER^{T2}-Igf2bp1$^{fl/fl}$* group. Age-matched (8–10-week) male and female *Villin-CreER^{T2}-Igf2bp1$^{fl/fl}$* ($n = 8$) and *Igf2bp1$^{fl/fl}$* ($n = 8$) mice were treated with 2% DSS in drinking water for 5 days followed by two additional cycles of 2% DSS with a 10–14-day interval between cycles. Mice were sacrificed on the 45th day of the experiment. *B*, percentage weight profile of mice during the experiment for chronic DSS treatment. *C*, DAI score plotted against time for chronic DSS treatment. *D*, representative pictures of colon and colon length comparison shown in the *top*. *Scale bar*, 25 mm. The lengths of age-matched female (14-16-week) *Villin-CreER^{T2}-Igf2bp1$^{fl/fl}$* ($n = 3$) and *Igf2bp1$^{fl/fl}$* ($n = 3$) mouse colons are quantified in the *bottom panel*. The data are mean ± S.D. (*error bars*). *E*, H&E-stained sections of colon from chronic DSS-treated *Villin-CreER^{T2}-Igf2bp1$^{fl/fl}$* mice showing severe loss of colonic surface epithelium and crypts when compared with control mice. *Scale bar*, 50 μm. *F*, histomorphological scores were plotted for H&E-stained colon sections from the chronic DSS experiment. Colon sections were scored by a pathologist who was blinded for sample identity. *, $p < 0.05$; **, $p < 0.01$; ***, $p < 0.001$.

Re-expression of occludin in IGF2BP1 deficient cells restores the tight-junction barrier function

Occludin plays an important role in the formation of the tight-junction seal by regulating macromolecule flux across the barrier (23, 26). To determine whether disregulation of occludin contributes to altered barrier function induced by down-regulation of IGF2BP1, we analyzed the permeability of Caco-2 cells grown as a monolayer. As predicted, IGF2BP1 knockdown resulted in decreased occludin expression in Caco-2 cells (Figs. 4*C* and 5*A*). To analyze the barrier, we grew Caco-2, with or without knockdown of IGF2BP1, on transwell plates. We found that IGF2BP1 knockdown caused a significant decrease in *trans*-epithelial electrical resistance (TER), indicating increased permeability in the Caco-2 monolayer (Fig. 5*B*). The TER levels were completely restored after re-expressing occludin in IGF2BP1 knockdown cells (Fig. 5*B*).

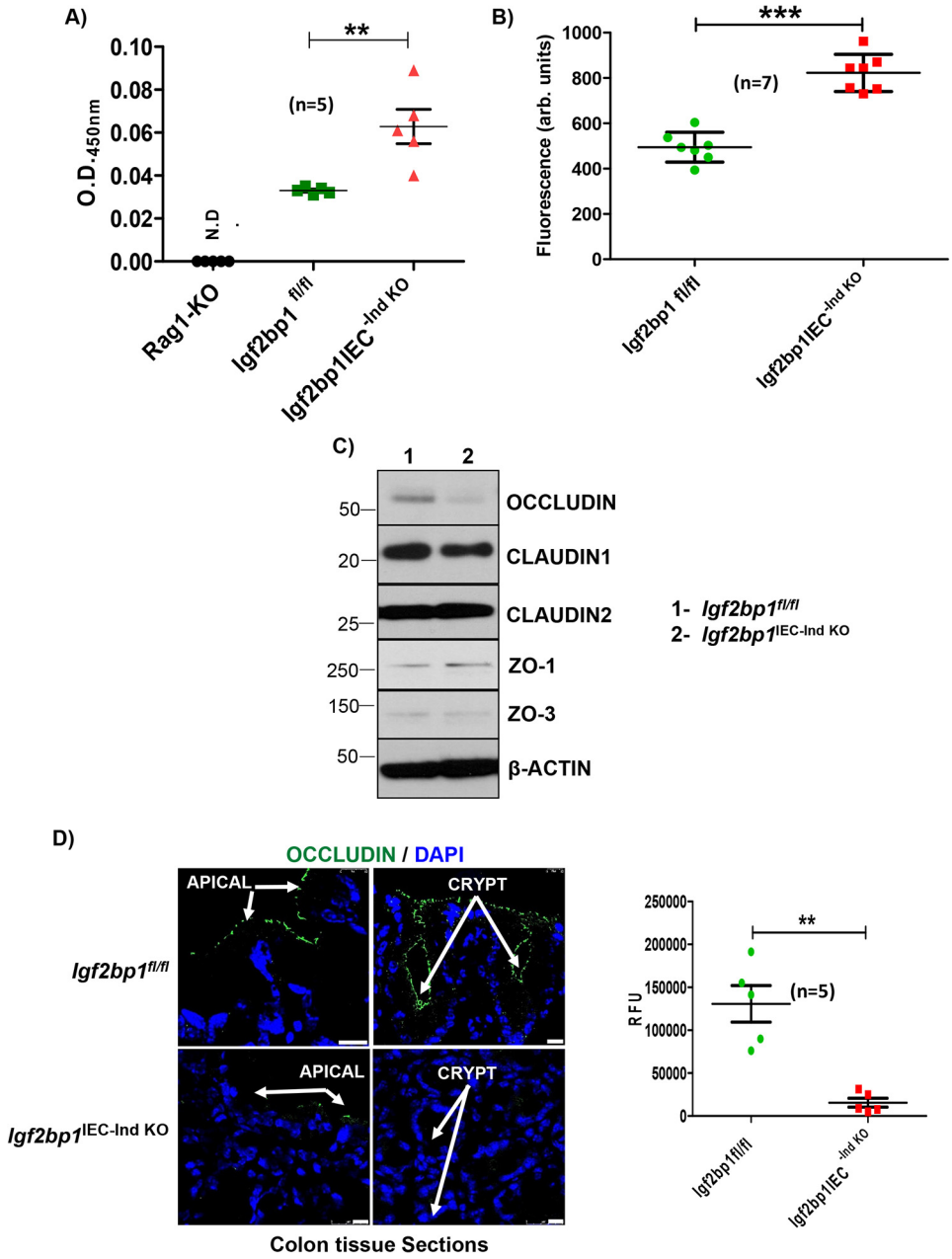

Figure 3. Deletion of IGF2BP1 from IECs increases the intestinal permeability in mice. *A*, LPS-specific IgG levels in the serum of *Villin-CreER^{T2}-Igf2bp1$^{fl/fl}$* ($n = 5$) and *Igf2bp1$^{fl/fl}$* ($n = 5$) mice. Rag1 knockout mice ($n = 5$) were taken as a negative experimental control. The data are means ± S.D. (*error bars*). *B*, analysis of intestinal epithelial permeability of mice by measuring FITC-dextran levels in the serum of mice *Villin-CreER^{T2}-Igf2bp1$^{fl/fl}$* ($n = 7$) and *Igf2bp1$^{fl/fl}$* ($n = 7$). The data are means ± S.D. *C*, immunoblot of tight-junction proteins in mouse intestinal epithelium (representative picture of three independent experiments). Shown is whole-cell extract from IECs of *Igf2bp1$^{fl/fl}$* ($n = 3$) and *Villin-CreER^{T2}-Igf2bp1$^{fl/fl}$* ($n = 3$) mice analyzed for occludin, CLAUDIN-1, CLAUDIN-2, ZO-1, and ZO-3 protein expression. β-Actin was evaluated as loading control. *D*, colon sections with occludin staining (*green*) showing the level of occludin expression in *Igf2bp1$^{fl/fl}$* ($n = 5$) and *Villin-CreER^{T2}-Igf2bp1$^{fl/fl}$* ($n = 3$) mice. *Scale bar*, 10 μm. Images are quantified for occludin by ImageJ software, and data are means ± S.D. **, $p < 0.01$; ***, $p < 0.001$. *N.D.*, not detected; *RFU*, relative fluorescence units.

We had also found increase flux in IGF2BP1 knockdown cells while this flux was restored after re-expression of occludin in IGF2BP1 knockdown cells (Fig. 5*C*).

Occludin knockout mice displayed retarded growth and chronically inflamed gastrointestinal tracts (35). Studies on *Ocln* knockout mice had revealed that occludin is an important factor in regulating the leak pathway in the mouse intestine (36–39). Our results demonstrate that deletion of *Igf2bp1* from intestinal epithelium leads to the disruption of occludin, which in turn increases the permeability of intestine. Re-expression of occludin restores the barrier function in the IGF2BP1-depleted monolayer of Caco-2 cells. These results suggest that IGF2BP1 maintains the intestinal barrier function at least partially by binding to and stabilizing occludin mRNAs.

The epithelial barrier function is required to maintain intestinal homeostasis, and any alterations contribute to diseases such as IBD (23). Actively inflamed tissue was found to be leaky in various studies (22). However, occludin was the only tight-junction protein found to be down-regulated even in nonactively inflamed tissue in ulcerative colitis (40). This supports

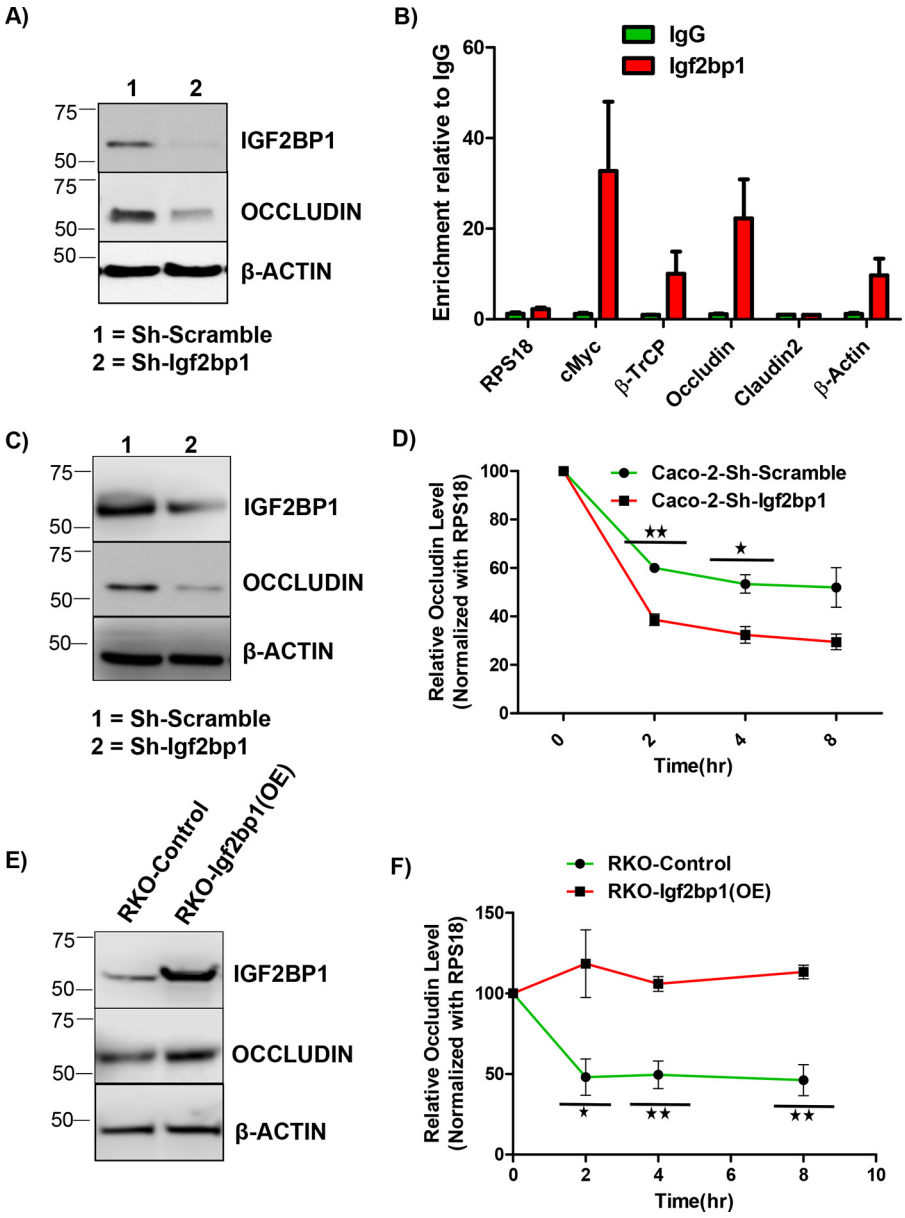

Figure 4. IGF2BP1 deletion alters the expression of tight-junction proteins. *A*, immunoblot analysis of occludin proteins. CCD-841-CoTr cells transduced with scramble or Igf2bp1-specific shRNA were analyzed for occludin protein expression. Igf2bp1 immunoblotting demonstrates the extent of knockdown. The picture is representative of three independent experiments. *β*-Actin was evaluated as a loading control. *B*, CLIP in CCD-841-CoTr cells shows -fold enrichment of the indicated RNA. RNAs were co-immunoprecipitated with anti-IGF2BP1 antibodies with an isotype IgG serving as a control. Two independent repeats were performed, and the data are representative of the mean of two repeats with *error bars* showing S.D. RPS18 was evaluated as a negative control, whereas *MYC* and *β-TRCP* served as positive controls. *C*, immunoblotting of Caco-2 cells transduced with scramble or Igf2bp1-specific shRNA with anti-occludin antibody. The anti-IGF2BP1 immunoblot shows the efficiency of IGF2BP1 knockdown. The picture shown is representative of three independent experiments. *β*-Actin was evaluated as loading control. *D*, mRNA degradation assay in Caco-2 cells transduced with doxycycline-inducible scramble or Igf2bp1-specific shRNA. Cells were grown for 4 days with doxycycline treatment to induce knockdown of IGF2BP1. Actinomycin D was added at time 0, and cell samples were collected at 0-, 2-, 4-, and 8-h time points from the same plate. Occludin mRNA levels were evaluated via quantitative RT-PCR. The data are means ± S.D. (*error bars*) of three independent experimental repeats. *E*, immunoblot analysis of occludin in RKO cells transduced with control or IGF2BP1 overexpression (Igf2bp1-OE) constructs. *β*-Actin was shown as loading control. *F*, the mRNA degradation assay in RKO cells transduced with control or IGF2BP1 overexpression (Igf2bp1-OE) constructs to show the stabilization of *OCLN* mRNA upon IGF2BP1 overexpression. Actinomycin D was treated at 0 h, and cells were collected at 0, 2, 4, and 8 h from the same plate. Total RNA was isolated followed by quantitative RT-PCR to analyze the occludin mRNA levels. *, $p < 0.05$; **, $p < 0.01$; ***, $p < 0.001$.

the importance of occludin in barrier function and disease. *OCLN* was shown to be regulated post-transcriptionally by RBPs and miRNAs (41, 42). The miRNA-429 and RBP CUGBP1 regulate *OCLN* negatively by binding to its 3′-UTR, whereas another RBP, HuR, regulates *OCLN* expression positively by binding to its 3′-UTR (25, 43). Our results provide further evidence for the importance of post-transcriptional regulation of *OCLN* mRNA at the level of mRNA stability. Interestingly, the reported miR-429–binding site (at positions 139-145 in the 3′-UTR of the *OCLN* mRNA) is in close proximity to one of the IGF2BP1 consensus-binding sequences, CA(A/U)(C/U)A (positions 133-137) (19). It is therefore plausible that

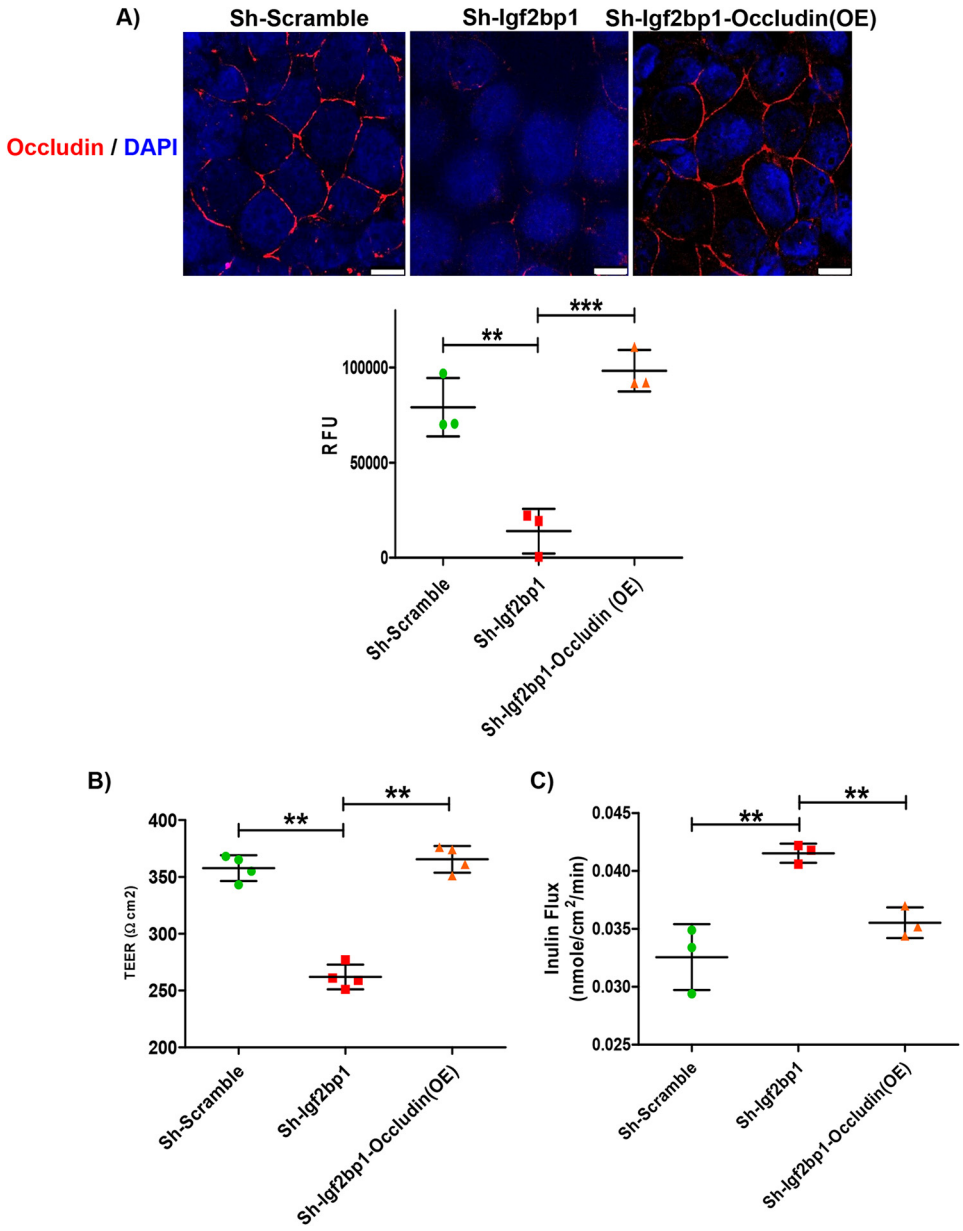

Figure 5. Restoration of barrier function upon re-expression of occludin. *A*, monolayer of Caco-2 cells, transduced as indicated, were stained with occludin (*red*) antibody. Five images, each from a different area of the same plate, were captured and quantified using ImageJ software. The data shown *below* the images represent three biological replicates. *Scale bar*, 10 μm. *B*, determination of paracellular permeability by TER. The TER was measured after growing Caco-2 cells transduced as indicated for 15 days in chambered plates. The data are mean ± S.D. ($n = 3$) with $p = 0.0030$ and $p = 0.0024$, respectively. *C*, the apical flux of the paracellular macromolecular probe, inulin (molecular radius, 15 Å) was measured and plotted for filter-grown Caco-2 cells transduced as indicated. **, $p < 0.01$; ***, $p < 0.001$; *RFU*, relative fluorescence units.

IGF2BP1 protects *OCLN* mRNA from microRNA-dependent degradation. This mechanism of action of IGF2BP1 has been reported previously for other IGF2BP1 targets (12, 13, 20, 44)

It is plausible that other targets of IGF2BP1 contribute to the observed intestinal phenotype. For example, knockout of one of the previously identified IGF2BP1 target genes, β-TrCP1 (14), together with heterozygous deletion of its paralog, Fbxw11, in mouse gut epithelium causes lethal mucosal inflammation (45); however, we did not observe significant changes in mRNA expression of β-TrCP1 and Fbxw11 genes in IECs *Igf2bp1*$^{\text{IEC-Ind KO}}$ mice compared with control littermates (Fig. S2, *B* and *C*). We also examined the expression level of Myc, another IGF2BP1 target gene, shown to maintain intestinal crypt numbers in juvenile mice (46), but we did not detect significant changes in the mRNA expression of Myc between control and *Igf2bp1*$^{\text{IEC-Ind KO}}$ mice (Fig. S2*A*).

Wnt signaling and its importance in maintaining stem cell populations in the intestinal crypts has been reviewed extensively by Gehart and Clevers (47). IGF2BP1 expression is transcriptionally regulated by Wnt/β-catenin signaling (14), and the mRNAs of several Wnt target genes (*e.g. MYC* and *MITF*) were shown to be stabilized by IGF2BP1 in various cancer cell lines (5, 13). These findings hint at a possible role that IGF2BP1 plays in supporting some functions of Wnt signaling and suggests that it might be a potentially important component of Wnt-regulated intestinal homeostasis.

Deletion of *Igf2bp1* from mouse intestinal epithelium has been shown to mitigate experimental colitis (31). Therefore, one might think that deletion of *Igf2bp1* would probably protect intestinal epithelial barrier function. However, our results show that Igf2bp1 loss exacerbates experimental colitis in mice, implying a protective role for this protein. The contrast in results could potentially be explained by the different knockout models used. Utilization of inducible knockouts in our studies is probably more relevant for modeling intestinal inflammation in adults, whereas constitutive knockouts used by Chatterji *et al.* (31) are more useful to model development of intestinal epithelia and intestinal abnormalities during childhood.

Our data imply that in adult animals, the IGF2BP1 regulates occludin and hence protects the barrier function of intestinal epithelia. The experimental data summarized in this article provide novel evidence indicating the importance of IGF2BP1 in post-transcriptional regulation of occludin, via regulating *OCLN* mRNA stability.

Experimental procedures

Cell culture and reagents

Normal human colon epithelium CCD-841-CoTr cells, human colon cancer RKO cells, and Caco-2 cells were cultured and maintained as monolayers in Dulbecco's modified Eagle's medium (VWR International), supplemented with 10% (v/v) fetal bovine serum (Gibco, Life Technologies, Inc.) and 100 units/ml penicillin and streptomycin (Corning). The cells were incubated at 37 °C, 5% CO_2. All cell lines were tested for mycoplasma contamination with the MycoAlert PLUS mycoplasma detection kit (Lonza).

Generation of IGF2BP1 knockdown, IGF2BP1 overexpression, and occludin expression cell lines

IGF2BP1 was knocked down using doxycycline-inducible shRNA constructs (purchased from GE Dharmacon). The *IGF2BP1* doxycycline-inducible overexpression lentiviral plasmid was constructed by cloning PCR-amplified human *IGF2BP1* ORF into the pInducer-20 vector (48). Lentivirus particles were produced from the above plasmids in Lenti-X 293T cells and were used to transduce CCD-CoTr, Caco-2, and RKO cells to make stable cell lines. Constitutively occludin-expressing Caco-2 cell lines in an IGF2BP1 knockdown background were constructed by transducing Caco-2-Sh-Igf2bp1 cells with pDUAL OCLN (GFP) lentiviral plasmid, which was gifted from Joe Grove (Addgene plasmid 86982; RRID:Addgene_86982).

Animals

Animals were maintained and procedures were performed in accordance with conditions approved by the Institutional Animal Care and Use Committee, Pennsylvania State University College of Medicine. *Villin*-CreER^{T2}-*Igf2bp1*$^{fl/fl}$ mice were generated by crossing *Villin-CreER*^{T2} (49) mice with *Igf2bp1*$^{f/fl}$ mice. *Igf2bp1*$^{fl/fl}$ mice were generated previously and maintained on C57Bl/6 background (50). The *Igf2bp1*$^{fl/fl}$ mice were used as experimental controls. To knock out *Igf2bp1*, *Villin-CreER*^{T2}-*Igf2bp1*$^{f/fl}$ mice were treated with a tamoxifen chow diet (Envigo-TD-130857) on weekdays, whereas a regular diet was given on weekends. *Igf2bp1*$^{f/fl}$ mice were also treated with tamoxifen chow in all experiment to serve as experimental control. During all animal experiments, *Igf2bp1*$^{fl/fl}$ and *Villin-CreER*^{T2}-*Igf2bp1*$^{fl/fl}$ mice were co-housed for the reproducibility of results and to avoid potential contribution of differences in microbiota in observed phenotypes (51).

Tissue staining

Colonic tissues were formalin-fixed, paraffin-embedded, and H&E-stained. Immunofluorescent and/or immunohistochemical staining was performed on frozen tissue sections as described (52). Imaging was performed at the Penn State Medical Center Cell Imaging Core. In brief, after blocking, the colon sections were incubated overnight with primary antibodies against occludin (Thermo Fisher OC-3F10). Fluorescence-labeled secondary antibodies (Jackson Laboratories) were used in conjunction with nuclear dye 4′,6-diamidino-2-phenylindole to visualize the distribution of occludin in the colon tissues. Images were quantified using ImageJ software.

Gut barrier assay

Relative levels of serum LPS-specific immunoreactivity were examined by ELISA, as described previously (53). Briefly, microtiter plates were coated with purified *Escherichia coli* LPS (2 μg/well; from *E. coli* 0128: B12, Sigma, catalog no. 2887). Serum samples were serially diluted 1:200, 1:600, and 1:1200 and applied to wells coated with LPS. After incubation and washing, the wells were incubated with anti-mouse IgG (1:1000) coupled to horseradish peroxidase. Immunoreactivity to LPS was captured using the colorimetric peroxidase substrate tetramethylbenzidine, and absorbance was read at 450 nm with the use of an ELISA plate reader. Data are reported as optical density corrected by subtracting background (determined by readings in blank samples). Serum samples from *Rag1*-deficient mice were used as negative controls.

DSS colitis

Sex- and age-matched littermates (8–10 weeks) received DSS (2%) in drinking water for 5 days. Mouse body weights were recorded daily. The disease activity index was determined as described (32). Mice that died or were euthanized prior to the study end point because of impaired condition were included in weight loss and DAI calculations where the data points were available.

In vivo epithelial permeability assay

The *in vivo* intestinal epithelial permeability was measured as described previously (54). Briefly, age- and sex-matched littermates were orally administered (0.6 mg/g of body weight) with FITC-dextran solution (4 kDa, 80 mg/ml). After 4 h, the mice were sacrificed, blood was obtained by cardiac puncture, and plasma was separated for determination of FITC by a fluorimeter at 488 nm.

In vitro permeability assay and determination of caco-2 paracellular permeability

Caco-2 cells were cultured on transwells with polyester membrane insert (Corning, 3421) allowing proper cellular polarization with formation of an apical (top compartment) and basolateral face (bottom compartment). The insert was pretreated with Dulbecco's modified Eagle's medium overnight before cell plating. Caco-2 cells were seeded at a density of 0.5×10^5 cells/insert. The medium was replaced with fresh medium every 2 days. The TER of the filter-grown Caco-2 cells was measured by an epithelial Voltohmmeter (World Precision Instruments, Sarasota, FL, USA). Beside the measurements of TER, Caco-2 paracellular permeability was determined using the inulin (−14 °C, M_r = 5000) as paracellular marker for the determination of apical flux rates. Known concentrations (1.5 μM) of this paracellular marker were added to the apical solution, and radioactivity was measured in basal solution using a scintillation counter, as described previously (55).

CLIP

CLIP was carried out with minor modifications in accordance with the previously published protocols (56, 57). Briefly, CCD 841 CoTr cells were cultured for 3 days and then fixed with 3% formaldehyde in PBS for 10 min followed by lysis through sonication (10 pulses for 10 s). Overnight immunoprecipitation was performed at 4 °C using anti-IGF2BP1 antibodies (MBL, catalog no. RN007P) linked to Dynabeads (Life Technologies, Inc.). After collection by magnetic separation and washing five times with lysis buffer, the RNA-protein complexes were reverse-cross-linked, and RNA was extracted using TRIzol reagent (Invitrogen) according to the manufacturer's instructions. Isolated RNA was treated with RNase-free DNase I (Thermo Scientific) to remove traces of genomic DNA. First-strand cDNA was generated using a cDNA synthesis kit from Bio-Rad according to the manufacturer's instructions, followed by real-time PCR using an iTaq Universal SYBR Green kit (Bio-Rad). The conditions for PCR amplification was as follows: initial denaturation for 3 minutes at 95°C, PCR amplification for 40 cycles with denaturation for the 20 seconds at 95°C, annealing for 20 seconds at 58°C and elongation at 72°C for 20 seconds. Analysis was done to obtain fold change in expression of particular gene by using CFX software from BioRad.

SDS-PAGE and immunoblotting analysis

Immunoblotting was done according to protocols described previously (58). Briefly, CCD-841-CoTr and Caco-2 cells were harvested, and whole-cell extract (WCE) was made by adding 1 ml of cell lysis buffer per 5×10^7 cells. The WCE was quantified using a Bio-Rad protein estimation kit. The WCE was analyzed by SDS-PAGE (10%) followed by immunoblotting. Blots were probed with the following antibodies: IGF2BP1, ZO-1, ZO-3, and β-actin from Cell Signaling, Claudin1 and occludin from Thermo Fisher, and Claudin2 from Abcam. Either anti-mouse or anti-rabbit horseradish peroxidase–conjugated secondary IgGs were used to detect their respective primary antibody. Quantitative luminescence of immunoblots was performed using ImageJ software.

Real-time PCR

Quantitative real-time PCR was conducted to quantify the mRNA levels. Total RNA was extracted using an RNeasy mini-kit from Qiagen, and cDNA was generated using an iScript cDNA synthesis kit (Bio-Rad) as per the manufacturer's instructions. Real-time PCR was performed using a CFX-96 RT-PCR machine with Bio-Rad SYBR Green mix. The conditions for PCR amplification were as follows: initial denaturation for 3 min at 95 °C, PCR amplification for 40 cycles with denaturation for the 20 s at 95 °C, annealing for 20 s at 58 °C, and elongation at 72 °C for 20 s. Analysis was done to obtain -fold change in expression of a particular gene by using CFX software from Bio-Rad. Three independent experiments were performed, and each sample was run in triplicate.

Data availability

All data relevant to these studies are contained within the article.

Acknowledgments—We thank Dr. Matam Vijay Kumar for invaluable input and suggestions to improve the manuscript. We also thank Dr. Joe Grove for the generous gift of reagent.

Author contributions—Vikash Singh and V. S. S. conceptualization; Vikash Singh, C. P. G., Vishal Singh, A. S. G., D. M. K., M. A. E., G. S. Y., P. N., and V. S. S. data curation; Vikash Singh, Vishal Singh, A. S. G., D. M. K., M. A. E., P. N., and V. S. S. formal analysis; Vikash Singh, C. P. G., A. S. G., G. S. Y., P. N., and V. S. S. validation; Vikash Singh, Vishal Singh, A. S. G., D. M. K., M. A. E., G. S. Y., and P. N. investigation; Vikash Singh, C. P. G., Vishal Singh, A. S. G., D. M. K., M. A. E., G. S. Y., P. N., and V. S. S. methodology; Vikash Singh writing-original draft; Vikash Singh, Vishal Singh, G. S. Y., P. N., and V. S. S. writing-review and editing; C. P. G., A. S. G., and D. M. K. visualization; G. S. Y. and V. S. S. resources; G. S. Y. and V. S. S. supervision; P. N. software; V. S. S. funding acquisition; V. S. S. project administration.

Funding and additional information—This study was supported in part by NCI, National Institutes of Health, Grants CA191550 and CA243167 (to V. S. S.). This work was also supported in part by NIDDK, National Institutes of Health, Grant DK114024 (to P. N.). The content is solely the responsibility of the authors and does not necessarily represent the official views of the National Institutes of Health.

Conflict of interest—The authors declare that they have no conflicts of interest with the contents of this article.

Abbreviations—The abbreviations used are: IGF2BP1, insulin-like growth factor 2 mRNA-binding protein 1; CLIP, cross-linking and RNA immunoprecipitation; IEC, intestinal epithelial cell; TJ, tight junction; IBD, inflammatory bowel disease; DSS, dextran sodium sulfate; DAI, disease activity index; RBP, RNA-binding protein; TER, trans-epithelial electrical resistance; miRNA, microRNA; shRNA, short hairpin RNA; WCE, whole-cell extract; H&E, hematoxylin and eosin; Ocln, occludin.

References

1. Degrauwe, N., Suva, M. L., Janiszewska, M., Riggi, N., and Stamenkovic, I. (2016) IMPs: an RNA-binding protein family that provides a link between stem cell maintenance in normal development and cancer. *Genes Dev.* **30,** 2459–2474 CrossRef Medline
2. Hansen, T. V., Hammer, N. A., Nielsen, J., Madsen, M., Dalbaeck, C., Wewer, U. M., Christiansen, J., and Nielsen, F. C. (2004) Dwarfism and impaired gut development in insulin-like growth factor II mRNA-binding protein 1-deficient mice. *Mol. Cell Biol.* **24,** 4448–4464 CrossRef Medline
3. Farina, K. L., Hüttelmaier, S., Musunuru, K., Darnell, R., and Singer, R. H. (2003) Two ZBP1 KH domains facilitate β-actin mRNA localization, granule formation, and cytoskeletal attachment. *J. Cell Biol.* **160,** 77–87 CrossRef Medline
4. Hüttelmaier, S., Zenklusen, D., Lederer, M., Dictenberg, J., Lorenz, M., Meng, X., Bassell, G. J., Condeelis, J., and Singer, R. H. (2005) Spatial regulation of β-actin translation by Src-dependent phosphorylation of ZBP1. *Nature* **438,** 512–515 CrossRef Medline
5. Leeds, P., Kren, B. T., Boylan, J. M., Betz, N. A., Steer, C. J., Gruppuso, P. A., and Ross, J. (1997) Developmental regulation of CRD-BP, an RNA-binding protein that stabilizes c-myc mRNA *in vitro*. *Oncogene* 14, 1279–1286 CrossRef Medline
6. Doyle, G. A., Betz, N. A., Leeds, P. F., Fleisig, A. J., Prokipcak, R. D., and Ross, J. (1998) The c-myc coding region determinant-binding protein: a member of a family of KH domain RNA-binding proteins. *Nucleic Acids Res* 26, 5036–5044 CrossRef Medline
7. Ross, A. F., Oleynikov, Y., Kislauskis, E. H., Taneja, K. L., and Singer, R. H. (1997) Characterization of a β-actin mRNA zipcode-binding protein. *Mol. Cell Biol.* **17,** 2158–2165 CrossRef Medline
8. Vikesaa, J., Hansen, T. V., Jønson, L., Borup, R., Wewer, U. M., Christiansen, J., and Nielsen, F. C. (2006) RNA-binding IMPs promote cell adhesion and invadopodia formation. *EMBO J.* **25,** 1456–1468 CrossRef Medline
9. Noubissi, F. K., Goswami, S., Sanek, N. A., Kawakami, K., Minamoto, T., Moser, A., Grinblat, Y., and Spiegelman, V. S. (2009) Wnt signaling stimulates transcriptional outcome of the Hedgehog pathway by stabilizing GLI1 mRNA. *Cancer Res.* **69,** 8572–8578 CrossRef Medline
10. Yisraeli, J. K. (2005) VICKZ proteins: a multi-talented family of regulatory RNA-binding proteins. *Biol. Cell* **97,** 87–96 CrossRef Medline
11. Manieri, N. A., Drylewicz, M. R., Miyoshi, H., and Stappenbeck, T. S. (2012) Igf2bp1 is required for full induction of Ptgs2 mRNA in colonic mesenchymal stem cells in mice. *Gastroenterology* **143,** 110–121.e110 CrossRef Medline
12. Elcheva, I., Goswami, S., Noubissi, F. K., and Spiegelman, V. S. (2009) CRD-BP protects the coding region of βTrCP1 mRNA from miR-183-mediated degradation. *Mol Cell* **35,** 240–246 CrossRef Medline
13. Goswami, S., Tarapore, R. S., Poenitzsch Strong, A. M., TeSlaa, J. J., Grinblat, Y., Setaluri, V., and Spiegelman, V. S. (2015) MicroRNA-340-mediated degradation of microphthalmia-associated transcription factor (MITF) mRNA is inhibited by coding region determinant-binding protein (CRD-BP). *J. Biol. Chem.* **290,** 384–395 CrossRef Medline
14. Noubissi, F. K., Elcheva, I., Bhatia, N., Shakoori, A., Ougolkov, A., Liu, J., Minamoto, T., Ross, J., Fuchs, S. Y., and Spiegelman, V. S. (2006) CRD-BP mediates stabilization of βTrCP1 and c-myc mRNA in response to β-catenin signalling. *Nature* **441,** 898–901 CrossRef Medline
15. Sparanese, D., and Lee, C. H. (2007) CRD-BP shields c-myc and MDR-1 RNA from endonucleolytic attack by a mammalian endoribonuclease. *Nucleic Acids Res.* **35,** 1209–1221 CrossRef Medline
16. Runge, S., Nielsen, F. C., Nielsen, J., Lykke-Andersen, J., Wewer, U. M., and Christiansen, J. (2000) H19 RNA binds four molecules of insulin-like growth factor II mRNA-binding protein. *J. Biol. Chem.* **275,** 29562–29569 CrossRef Medline
17. Gu, W., Katz, Z., Wu, B., Park, H. Y., Li, D., Lin, S., Wells, A. L., and Singer, R. H. (2012) Regulation of local expression of cell adhesion and motility-related mRNAs in breast cancer cells by IMP1/ZBP1. *J. Cell Sci.* **125,** 81–91 CrossRef Medline
18. Hafner, M., Landthaler, M., Burger, L., Khorshid, M., Hausser, J., Berninger, P., Rothballer, A., Ascano, M., Jr., Jungkamp, A. C., Munschauer, M., Ulrich, A., Wardle, G. S., Dewell, S., Zavolan, M., and Tuschl, T. (2010) Transcriptome-wide identification of RNA-binding protein and microRNA target sites by PAR-CLIP. *Cell* **141,** 129–141 CrossRef Medline
19. Conway, A. E., Van Nostrand, E. L., Pratt, G. A., Aigner, S., Wilbert, M. L., Sundararaman, B., Freese, P., Lambert, N. J., Sathe, S., Liang, T. Y., Essex, A., Landais, S., Burge, C. B., Jones, D. L., and Yeo, G. W. (2016) Enhanced CLIP uncovers IMP protein-RNA targets in human pluripotent stem cells important for cell adhesion and survival. *Cell Rep.* **15,** 666–679 CrossRef Medline
20. Müller, S., Glaë, M., Singh, A. K., Haase, J., Bley, N., Fuchs, T., Lederer, M., Dahl, A., Huang, H., Chen, J., Posern, G., and Hüttelmaier, S. (2019) IGF2BP1 promotes SRF-dependent transcription in cancer in a m6A- and miRNA-dependent manner. *Nucleic Acids Res.* **47,** 375–390 CrossRef Medline
21. Huang, H., Weng, H., Sun, W., Qin, X., Shi, H., Wu, H., Zhao, B. S., Mesquita, A., Liu, C., Yuan, C. L., Hu, Y. C., Hüttelmaier, S., Skibbe, J. R., Su, R., Deng, X., *et al.* (2018) Recognition of RNA N^6-methyladenosine by IGF2BP proteins enhances mRNA stability and translation. *Nat. Cell Biol.* **20,** 285–295 CrossRef Medline
22. Peterson, L. W., and Artis, D. (2014) Intestinal epithelial cells: regulators of barrier function and immune homeostasis. *Nature reviews. Immunology* **14,** 141–153 CrossRef Medline
23. Turner, J. R. (2009) Intestinal mucosal barrier function in health and disease. *Nature reviews. Immunology* **9,** 799–809 CrossRef Medline
24. Marchiando, A. M., Graham, W. V., and Turner, J. R. (2010) Epithelial barriers in homeostasis and disease. *Annual review of pathology* **5,** 119–144 CrossRef Medline
25. Yu, T. X., Rao, J. N., Zou, T., Liu, L., Xiao, L., Ouyang, M., Cao, S., Gorospe, M., and Wang, J. Y. (2013) Competitive binding of CUGBP1 and HuR to occludin mRNA controls its translation and modulates epithelial barrier function. *Mol. Biol. Cell* **24,** 85–99 CrossRef Medline
26. Cummins, P. M. (2012) Occludin: one protein, many forms. *Mol. Cell. Biol.* **32,** 242–250 CrossRef Medline
27. Kim, D. H., and Cheon, J. H. (2017) Pathogenesis of inflammatory bowel disease and recent advances in biologic therapies. *Immune Netw.* **17,** 25–40 CrossRef Medline
28. Rutgeerts, P., Vermeire, S., and Van Assche, G. (2009) Biological therapies for inflammatory bowel diseases. *Gastroenterology* **136,** 1182–1197 CrossRef Medline
29. Abraham, C., and Cho, J. H. (2009) Inflammatory bowel disease. *N. Engl. J. Med.* **361,** 2066–2078 CrossRef Medline
30. Hamilton, K. E., Chatterji, P., Lundsmith, E. T., Andres, S. F., Giroux, V., Hicks, P. D., Noubissi, F. K., Spiegelman, V. S., and Rustgi, A. K. (2015) Loss of stromal IMP1 promotes a tumorigenic microenvironment in the colon. *Mol. Cancer Res.* **13,** 1478–1486 CrossRef Medline
31. Chatterji, P., Williams, P. A., Whelan, K. A., Samper, F. C., Andres, S. F., Simon, L. A., Parham, L. R., Mizuno, R., Lundsmith, E. T., Lee, D. S., Liang, S., Wijeratne, H. S., Marti, S., Chau, L., Giroux, V., *et al.* (2019) Posttranscriptional regulation of colonic epithelial repair by RNA binding protein IMP1/IGF2BP1. *EMBO Rep.* **20** CrossRef
32. Rath, E., Berger, E., Messlik, A., Nunes, T., Liu, B., Kim, S. C., Hoogenraad, N., Sans, M., Sartor, R. B., and Haller, D. (2012) Induction of dsRNA-activated protein kinase links mitochondrial unfolded protein response to the pathogenesis of intestinal inflammation. *Gut* **61,** 1269–1278 CrossRef Medline
33. Wirtz, S., Neufert, C., Weigmann, B., and Neurath, M. F. (2007) Chemically induced mouse models of intestinal inflammation. *Nat. Protoc.* **2,** 541–546 CrossRef Medline
34. Catalioto, R. M., Maggi, C. A., and Giuliani, S. (2011) Intestinal epithelial barrier dysfunction in disease and possible therapeutical interventions. *Curr. Med. Chem.* **18,** 398–426 CrossRef Medline
35. Saitou, M., Furuse, M., Sasaki, H., Schulzke, J. D., Fromm, M., Takano, H., Noda, T., and Tsukita, S. (2000) Complex phenotype of mice lacking occludin, a component of tight junction strands. *Molecular biology of the cell* **11,** 4131–4142 CrossRef Medline
36. Al-Sadi, R., Khatib, K., Guo, S., Ye, D., Youssef, M., and Ma, T. (2011) Occludin regulates macromolecule flux across the intestinal epithelial tight junction barrier. *Am. J. Physiol. Gastrointest. Liver Physiol.* **300,** G1054–G1064 CrossRef Medline

37. Van Itallie, C. M., Fanning, A. S., Holmes, J., and Anderson, J. M. (2010) Occludin is required for cytokine-induced regulation of tight junction barriers. *J. Cell Sci*. **123,** 2844–2852 CrossRef Medline
38. Marchiando, A. M., Shen, L., Graham, W. V., Weber, C. R., Schwarz, B. T., Austin, J. R., 2nd, Raleigh, D. R., Guan, Y., Watson, A. J., Montrose, M. H., and Turner, J. R. (2010) Caveolin-1-dependent occludin endocytosis is required for TNF-induced tight junction regulation *in vivo*. *J. Cell Biol*. **189,** 111–126 CrossRef Medline
39. Buschmann, M. M., Shen, L., Rajapakse, H., Raleigh, D. R., Wang, Y., Wang, Y., Lingaraju, A., Zha, J., Abbott, E., McAuley, E. M., Breskin, L. A., Wu, L., Anderson, K., Turner, J. R., and Weber, C. R. (2013) Occludin OCEL-domain interactions are required for maintenance and regulation of the tight junction barrier to macromolecular flux. *Mol. Biol. Cell* **24,** 3056–3068 CrossRef Medline
40. Feldman, G. J., Mullin, J. M., and Ryan, M. P. (2005) Occludin: structure, function and regulation. *Adv. Drug Deliv. Rev*. **57,** 883–917 CrossRef Medline
41. Martinez, C., Rodino-Janeiro, B. K., Lobo, B., Stanifer, M. L., Klaus, B., Granzow, M., Gonzalez-Castro, A. M., Salvo-Romero, E., Alonso-Cotoner, C., Pigrau, M., Roeth, R., Rappold, G., Huber, W., Gonzalez-Silos, R., Lorenzo, J., *et al.* (2017) miR-16 and miR-125b are involved in barrier function dysregulation through the modulation of claudin-2 and cingulin expression in the jejunum in IBS with diarrhoea. *Gut* **66,** 1537–1538 CrossRef Medline
42. Xiao, L., and Wang, J. Y. (2014) RNA-binding proteins and microRNAs in gastrointestinal epithelial homeostasis and diseases. *Curr. Opin. Pharmacol*. **19,** 46–53 CrossRef Medline
43. Yu, T., Lu, X. J., Li, J. Y., Shan, T. D., Huang, C. Z., Ouyang, H., Yang, H. S., Xu, J. H., Zhong, W., Xia, Z. S., and Chen, Q. K. (2016) Overexpression of miR-429 impairs intestinal barrier function in diabetic mice by down-regulating occludin expression. *Cell Tissue Res*. **366,** 341–352 CrossRef Medline
44. Müller, S., Bley, N., Glaë, M., Busch, B., Rousseau, V., Misiak, D., Fuchs, T., Lederer, M., and Hüttelmaier, S. (2018) IGF2BP1 enhances an aggressive tumor cell phenotype by impairing miRNA-directed downregulation of oncogenic factors. *Nucleic Acids Res*. **46,** 6285–6303 CrossRef Medline
45. Kanarek, N., Grivennikov, S. I., Leshets, M., Lasry, A., Alkalay, I., Horwitz, E., Shaul, Y. D., Stachler, M., Voronov, E., Apte, R. N., Pagano, M., Pikarsky, E., Karin, M., Ghosh, S., and Ben-Neriah, Y. (2014) Critical role for IL-1β in DNA damage-induced mucositis. *Proc. Natl. Acad. Sci. U.S.A*. **111,** E702–E711 CrossRef Medline
46. Bettess, M. D., Dubois, N., Murphy, M. J., Dubey, C., Roger, C., Robine, S., and Trumpp, A. (2005) c-Myc is required for the formation of intestinal crypts but dispensable for homeostasis of the adult intestinal epithelium. *Mol. Cell. Biol*. **25,** 7868–7878 CrossRef Medline
47. Gehart, H., and Clevers, H. (2019) Tales from the crypt: new insights into intestinal stem cells. *Nat. Rev. Gastroenterol. Hepatol*. **16,** 19–34 CrossRef Medline
48. Meerbrey, K. L., Hu, G., Kessler, J. D., Roarty, K., Li, M. Z., Fang, J. E., Herschkowitz, J. I., Burrows, A. E., Ciccia, A., Sun, T., Schmitt, E. M., Bernardi, R. J., Fu, X., Bland, C. S., Cooper, T. A. *et al.* (2011) The pINDUCER lentiviral toolkit for inducible RNA interference *in vitro* and *in vivo*. *Proc. Natl. Acad. Sci. U.S.A*. **108,** 3665–3670 CrossRef Medline
49. el Marjou, F., Janssen, K. P., Chang, B. H., Li, M., Hindie, V., Chan, L., Louvard, D., Chambon, P., Metzger, D., and Robine, S. (2004) Tissue-specific and inducible Cre-mediated recombination in the gut epithelium. *Genesis* **39,** 186–193 CrossRef Medline
50. Hamilton, K. E., Noubissi, F. K., Katti, P. S., Hahn, C. M., Davey, S. R., Lundsmith, E. T., Klein-Szanto, A. J., Rhim, A. D., Spiegelman, V. S., and Rustgi, A. K. (2013) IMP1 promotes tumor growth, dissemination and a tumor-initiating cell phenotype in colorectal cancer cell xenografts. *Carcinogenesis* **34,** 2647–2654 CrossRef Medline
51. Franklin, C. L., and Ericsson, A. C. (2017) Microbiota and reproducibility of rodent models. *Lab Anim*. **46,** 114–122 CrossRef Medline
52. Chen, Y., Zhang, H. S., Fong, G. H., Xi, Q. L., Wu, G. H., Bai, C. G., Ling, Z. Q., Fan, L., Xu, Y. M., Qin, Y. Q., Yuan, T. L., Sun, H., and Fang, J. (2015) PHD3 stabilizes the tight junction protein occludin and protects intestinal epithelial barrier function. *J. Biol. Chem*. **290,** 20580–20589 CrossRef Medline
53. Ziegler, T. R., Luo, M., Estivariz, C. F., Moore, D. A., 3rd, Sitaraman, S. V., Hao, L., Bazargan, N., Klapproth, J. M., Tian, J., Galloway, J. R., Leader, L. M., Jones, D. P., and Gewirtz, A. T. (2008) Detectable serum flagellin and lipopolysaccharide and upregulated anti-flagellin and lipopolysaccharide immunoglobulins in human short bowel syndrome. *Am. J. Physiol. Regul. Integr. Comp. Physiol*. **294,** R402–R410 CrossRef Medline
54. Tambuwala, M. M., Cummins, E. P., Lenihan, C. R., Kiss, J., Stauch, M., Scholz, C. C., Fraisl, P., Lasitschka, F., Mollenhauer, M., Saunders, S. P., Maxwell, P. H., Carmeliet, P., Fallon, P. G., Schneider, M., and Taylor, C. T. (2010) Loss of prolyl hydroxylase-1 protects against colitis through reduced epithelial cell apoptosis and increased barrier function. *Gastroenterology* **139,** 2093–2101 CrossRef Medline
55. Nighot, P. K., Hu, C. A., and Ma, T. Y. (2015) Autophagy enhances intestinal epithelial tight junction barrier function by targeting claudin-2 protein degradation. *J. Biol. Chem*. **290,** 7234–7246 CrossRef Medline
56. Vogt, M., and Taylor, V. (2013) Cross-linked RNA immunoprecipitation. *Bio-protoc*. **3,** e398 CrossRef
57. Knuckles, P., Vogt, M. A., Lugert, S., Milo, M., Chong, M. M., Hautbergue, G. M., Wilson, S. A., Littman, D. R., and Taylor, V. (2012) Drosha regulates neurogenesis by controlling neurogenin 2 expression independent of microRNAs. *Nat. Neurosci*. **15,** 962–969 CrossRef Medline
58. Harlow, E. (1988) Immunoblotting. in *Antibodies: A Laboratory Manual* (Harlow, H., and Lane, D., eds) pp. 471–510, Cold Spring Harbor Laboratory Press, Cold Spring Harbor, NY
59. Erben, U., Loddenkemper, C., Doerfel, K., Spieckermann, S., Haller, D., Heimesaat, M. M., Zeitz, M., Siegmund, B., and Kühl, A. A. (2014) A guide to histomorphological evaluation of intestinal inflammation in mouse models. *Int. J. Clin. Exp. Pathol*. **7,** 4557–4576 Medline